CASE REPORT

Clonal evidence for the development of neuroblastoma with extensive copy-neutral loss of heterozygosity arising in a mature teratoma

Rintaro Ono[1] 🆔 | Hiroo Ueno[2] | Kenichi Yoshida[2] | Satoko Takahashi[1,3] | Hiroki Yoshihara[1] | Taiki Nozaki[4] | Koyu Suzuki[5] | Atsuko Nakazawa[6] | Ryunosuke Saiki[2] | Masafumi Seki[7] | Junko Takita[7,8] | Seishi Ogawa[2] | Atsushi Manabe[1,9] | Daisuke Hasegawa[1]

[1]Department of Pediatrics, St. Luke's International Hospital, Tokyo, Japan

[2]Department of Pathology and Tumor Biology, Graduate School of Medicine, Kyoto University, Kyoto, Japan

[3]Department of Pediatrics, Japanese Red Cross Narita Hospital, Chiba, Japan

[4]Department of Diagnostic Radiology, St. Luke's International Hospital, Tokyo, Japan

[5]Department of Pathology, St. Luke's International Hospital, Tokyo, Japan

[6]Department of Clinical Research, Saitama Children's Medical Center, Saitama, Japan

[7]Department of Pediatrics, Graduate School of Medicine, The University of Tokyo, Tokyo, Japan

[8]Department of Pediatrics, Graduate School of Medicine, Kyoto University, Kyoto, Japan

[9]Department of Pediatrics, Hokkaido University Graduate School of Medicine, Sapporo, Japan

Correspondence
Daisuke Hasegawa, Department of Pediatrics, St Luke's International Hospital, 9-1 Akashicho, Chuo-ku, Tokyo 104-0044, Japan.
Email: hasedai1313@gmail.com

Abstract

Mature teratomas are usually benign tumors that rarely undergo malignant transformation. We report an advanced neuroblastoma arising in a mature teratoma of the ovary. Whole-exome sequencing identified extensive copy-neutral loss of heterozygosity (LOH) in both neuroblastoma and teratoma elements, suggesting that the neuroblastoma evolved from the teratoma. In addition, several truncating germline heterozygous variants in tumor suppressor genes, including *RBL2* and *FBXW12*, became homozygous as a result of LOH. Collectively, we speculate that extensive LOH in teratoma cells may force heterozygous germline variants to become homozygous, which, in turn, may contribute to the development of neuroblastoma with the acquisition of additional chromosomal changes.

KEYWORDS

cancer genome/genetics, copy-neutral loss of heterozygosity, genomic analysis, malignant transformation, neuroblastoma, teratoma

1 | INTRODUCTION

A mature teratoma is a subtype of a germ cell tumor that occurs in both adults and children. Most cases of mature teratomas are benign, and malignant transformation rarely occurs.[1] Although carcinomas are common malignancies arising in mature teratomas, embryonal malignancies, including neuroblastoma, can also occur.[2] Previous studies have shown additional somatic mutations in genes such as *TP53*, *PIK3CA*, and *CDKN2A* during malignant transformation in squamous cell carcinoma and adenocarcinoma.[3] However, genetic changes that contribute to the malignant transformation of teratoma to neuroblastoma and their clonal relationship have not been previously reported.

Neuroblastoma is an embryonal malignant tumor originating from the sympathetic nervous system. It is the most common type of extracranial malignant tumor in children, and over 90% cases of neuroblastoma are found in children younger than 10 y of age. Neuroblastoma in adolescents and young adults (AYA) is rare, often showing an indolent course and poor prognosis.[4]

Here, we report a 15-y-old girl with neuroblastoma arising in a mature cystic teratoma of the ovary who was successfully treated using a multidisciplinary treatment approach. We identified the underlying genetic changes within the elements of the mature cystic teratoma and neuroblastoma using whole-exome sequencing and copy number analysis.

2 | MATERIALS AND METHODS

2.1 | Pathological diagnosis and DNA extraction

After surgical resection, samples were immediately fixed with formaldehyde. FFPE sections were prepared from different tumor regions, and pathological evaluation was performed. For genetic analysis, neuroblastoma-enriched lesions and teratoma-enriched lesions were pathologically reviewed using the respective FFPE sections to identify tissue regions for DNA extraction. At 8 mo after tumor resection, samples cut from the paraffin block, as well as peripheral blood, underwent DNA extraction using a GeneRead DNA FFPE Kit and DNeasy Blood & Tissue Kit (Qiagen), respectively, in accordance with the manufacturer's instructions.

2.2 | Whole-exome sequencing

DNA libraries were prepared using SureSelect Human All Exon V5 (Agilent Technologies) in accordance with the manufacturer's instructions. Enriched exome libraries were sequenced on an Illumina HiSeq 2500 instrument. Somatic variants were called using Genomon v.2.3.0 with the following parameters: (a) VAFs < 0.05 in normal samples, (b) Empirical Bayesian Mutation Calling $P \geq .0001$, and (c) variants not only present in unidirectional reads. Mapping errors were removed by visual inspection using the Integrative Genomics Viewer

tool. To narrow down the disease-causing candidate germline variants, mutations with frequencies in the normal population <1% and VAFs in peripheral blood >0.2 were selected. Mapping errors were also removed by visual inspection on the Integrative Genomics Viewer browser (http://www.broadinstitute.org/igv/).

2.3 | Copy number analysis

Allele-specific copy numbers were calculated by allele frequencies and sequenced depths of single nucleotide polymorphisms using our in-house CNACS pipeline, the scripts of which are available at https://github.com/papaemmelab/toil_cnacs.

2.4 | Ethics approval and consent to the study

This study was reviewed and approved by the Institutional Review Board of St. Luke's International Hospital, Kyoto University, and the University of Tokyo. Written informed consent was obtained from the patient and her parents.

2.5 | Data availability

Sequencing data were deposited at the European Genome-phenome Archive (http://www.ebi.ac.uk/ega/) under the accession number EGAS00001005116.

3 | RESULTS

3.1 | Case presentation

A 15-y-old girl complained of lumbar pain and abdominal distention for 1 mo. Contrast-enhanced MRI and computed tomography showed a bulky solid mass with heterogeneous enhancement, measuring 11 × 9 × 11 cm, in the left ovary (Figure S1A-E). The tumor consisted of cystic and solid components, including calcification and minimal fat. Mediastinal and para-aortic lymphadenopathies were also observed. Left salpingo-oophorectomy, partial omentectomy, and pelvic and para-aortic lymphadenectomy were performed, although para-aortic lymph nodes were partially unresectable. Histopathological examination revealed that the tumor consisted of 10% teratoma elements and 90% neuroblastoma elements (Figure 1A-C). The teratoma component contained tissues derived from all 3 germ layers, thereby characterized as a mature cystic teratoma. By contrast, the neuroblastoma component was mainly composed of poorly differentiated, dense, chromatin-rich small round cells with a low mitosis-karyorrhexis index. Immunohistochemistry of neuroblastoma elements showed cells positive for anti-synaptophysin, anti-chromogranin, and tyrosine hydroxylase. The DNA index was diploidy, and *MYCN* was not amplified. Evaluation
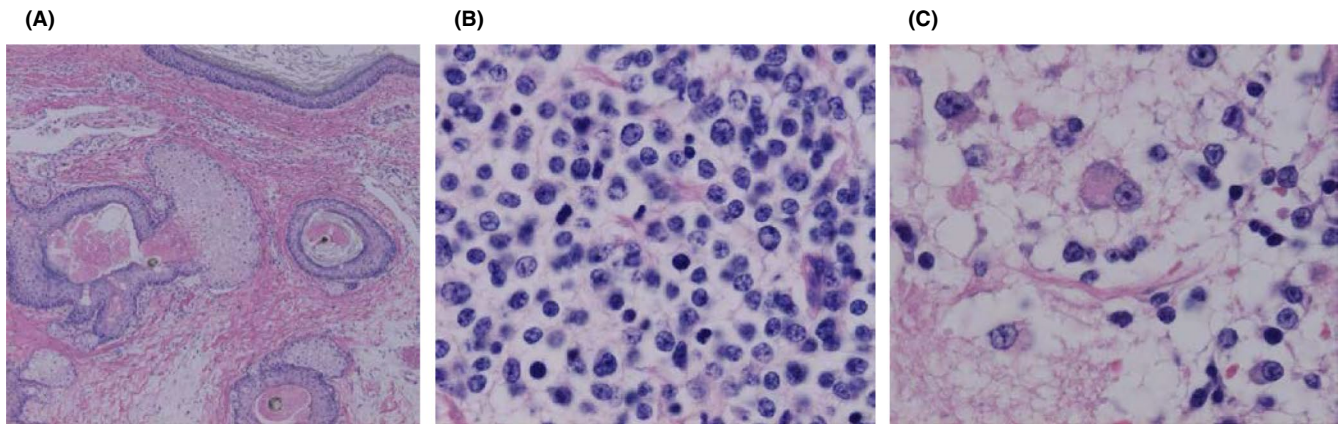
FIGURE 1 Histopathological evaluation of ovarian tumor. A-C, H&E staining of the tumor. Neuroblastomatous tissue consisting of dense, solid proliferation of small round cells with increased chromatin. There are minor components with multilayered squamous epithelium with skin appendage-like structures and choriocapillary epithelium

of the para-aortic lymph node showed similar findings to the neuroblastoma component. Bone marrow aspiration showed metastasis of neuroblastoma cells positive for NSE. Cytogenetic analysis showed 45,X,−X,+1,der(1;8)(q10;q10),del(9)(q?),add(11)(p15),der(14;22) (q10;q10),+17 in 4 of 20 cells analyzed. Both bone scintigraphy and MIBG scintigraphy showed no abnormal uptake of radioactive tracers. Serum NSE was elevated (up to 129 ng/mL), but urine catecholamine metabolites did not increase. On the basis of these findings, we diagnosed the patient with neuroblastoma arising in a mature teratoma of the left ovary with multiple metastases.

Mediastinal and para-aortic lymphadenopathies progressed rapidly 1 wk after surgery, leading to a compressed ureter and hydronephrosis (Figure S2A,B). After confirming normal renal function, multiagent chemotherapy for neuroblastoma, consisting of cyclophosphamide (1200 mg/m^2/d, day 1 for the 1st course; days 1-2 for subsequent courses), vincristine (1.5 mg/m^2/d, day 1), pirarubicin (40 mg/m^2/d, day 3), and cisplatin (20 mg/m^2/d, days 1-5), was initiated. Chemotherapy successfully reduced the size of the metastatic lymph nodes, and serum NSE was reduced to 15.7 ng/mL 2 wk after the initiation of treatment. After 5 courses of chemotherapy, we administered high-dose chemotherapy, consisting of busulfan (3.2 mg/kg/d, days −6 to −3) and melphalan (140 mg/m^2/d, day −2), followed by autologous peripheral blood stem cell rescue. Neutrophil engraftment was achieved on day 12 after transplantation, and she did not develop transplant-related complications. The patient underwent lymphadenectomy of residual para-aortic lymph nodes on day 48 from transplantation, showing no viable cells. She received 19.8 Gy of local irradiation to the mediastinum and retroperitoneum, followed by 9 courses of 13-*cis*-retinoic acid. At 9 y after diagnosis, she is alive without any evidence of disease recurrence.

3.2 | Genomic analysis of neuroblastoma- and teratoma-enriched elements

To identify genetic abnormalities that may facilitate malignant transformation and to determine the clonal relationship between teratoma and neuroblastoma, we performed whole-exome sequencing using DNA extracted from neuroblastoma-enriched lesions and mature teratoma-enriched lesions, as well as peripheral blood.

Table 1 shows the 14 somatic mutations and representative germline variants. Although 14 genes including *ARHGEF1* and *KCNJ10*, whose expression changes were reported in neuroblastoma cell lines[5,6] were mutated, no mutations were found in neuroblastoma driver genes such as *ALK* and *ATRX*. In total 11 of the 14 somatic mutations found in the neuroblastoma-enriched lesions were also found in the teratoma-enriched lesions with a low allele frequencies of <4% (Table 1), a finding that was in agreement with the histopathological finding that the teratoma lesions contained ~1%-5% of neuroblastoma components. Therefore, we concluded that no somatic mutations were identified in teratoma lesions.

Next, we then evaluated copy number alterations in neuroblastoma-enriched lesions and teratoma-enriched lesions, as well as peripheral blood by a sequencing-based method. Although no copy number alterations were found in peripheral blood (Figure 2A, upper panel), teratoma-enriched lesions showed genome-wide CN-LOH, which is also known as uniparental disomy (UPD) (Figure 2A, middle panel).[7-9] Intriguingly, the neuroblastoma-enriched lesions also showed genome-wide CN-LOH, suggesting that the neuroblastoma cells were derived from the teratoma cells. The neuroblastoma-enriched lesions also showed additional copy number alterations including +1q, +17, and −X, which are characteristic of neuroblastoma (Figure 2A, lower panel).

The extensive CN-LOH in teratoma and neuroblastoma indicates that heterozygous germline variants would become homozygous in tumor cells, otherwise heterozygous germline variants would be lost and become wild-type. Therefore, we next investigated whether the neuroblastoma harbored germline variants that became homozygous when CN-LOH occurred. Of 478 rare germline variants detected in a peripheral blood sample, 248 heterozygous variants, including loss-of-function mutations in *EZH2*, *FBXW12*, and *RBL2*, showed VAFs of nearly 1.0 (0.97 ± 0.03) in neuroblastoma-enriched lesions suggesting that these variants became homozygous, while the remaining

TABLE 1 Somatic mutations and representative germline single nucleotide variants in peripheral blood, neuroblastoma-enriched lesions, and teratoma-enriched lesions

Type	Gene	Exonic function	Amino acid change	VAF (neuroblastoma-enriched lesions)	VAF (teratoma-enriched lesions)	VAF (peripheral blood)
Somatic	ANKRD31	Nonsynonymous SNV	L604P	0.42	0.01	0.00
	ARHGEF1	Nonsynonymous SNV	T662M	0.52	0.04	0.00
	CNBP	Synonymous SNV	Q98Q	0.36	0.00	0.00
	CNGA3	Nonsynonymous SNV	D199V	0.60	0.06	0.00
	DHX34	Synonymous SNV	L138L	0.37	0.03	0.00
	GRAP2	Nonsynonymous SNV	N192K	0.41	0.04	0.00
	INO80D	Frameshift deletion	868_895del	0.24	0.01	0.00
	KCNJ10	Nonsynonymous SNV	R26G	0.07	0.00	0.00
	KDM4E	Synonymous SNV	P327P	0.45	0.00	0.00
	KIAA1217	Nonsynonymous SNV	A539S	0.50	0.02	0.00
	P2RY2	Nonsynonymous SNV	S141F	0.44	0.05	0.00
	SH3TC1	Nonsynonymous SNV	A282S	0.45	0.01	0.00
	SVIL	Nonsynonymous SNV	E1545K	0.40	0.02	0.00
	ZKSCAN3	Nonsynonymous SNV	V27M	0.46	0.04	0.00
Germline	RBL2	Stop gain	K911X	0.95	0.90	0.51
	FBXW12	Frameshift deletion	N353fs	1.00	0.70	0.50
	EZH2	Splice site	1547-2A>C	0.99	0.68	0.40

230 heterozygous variants showed VAFs of nearly 0.0 (0.02 ± 0.02) suggesting that these became wild-type in neuroblastoma-enriched lesions (Table 1 and Dataset S1). Conversely, VAFs of mature-teratoma-enriched lesions showed less contrast when relevant 248 and 230 variants were 0.69 ± 0.09 and 0.27 ± 0.07, respectively. Figure 2B shows histograms of VAFs of 478 germline variants in mature teratoma-enriched lesions (Figure 2B, upper panel) and in neuroblastoma-enriched lesions (Figure 2B, lower panel). Although the possibility remains that the discrepancy of VAFs was due to heterogeneity of teratoma component, we suspect that it is more likely to be caused by contamination of normal tissue in teratoma-enriched lesions.

4 | DISCUSSION

Neuroblastoma occurring in AYA tends to show an indolent course with less sensitivity to chemotherapy compared with neuroblastoma in infants and young children. Genetic changes in neuroblastoma of AYA have a lower frequency of MYCN amplification and higher frequency of ALK and ATRX mutation, which are in contrast with neuroblastoma in infants and young children, and suggests that the

pathobiology of neuroblastoma may be different based on the age of onset.[4,10]

To date, 18 female cases of ovarian neuroblastoma have been reported (Table S1), of which 13 arose from teratomas. Here, 6 of these 13 teratoma-derived cases of neuroblastoma were advanced. Although the prognostic significance of a teratomatous component and treatment modalities were inconclusive because of the limited number of patients, local therapy without chemotherapy appears to be insufficient for patients with advanced disease. Despite the rapid progression of metastatic lymph nodes, our presented patient responded well to chemotherapy, and she remains in long-term remission after multidisciplinary treatment, including high-dose chemotherapy.

We performed whole-exome sequencing and sequencing-based copy number analysis of neuroblastoma-enriched lesions and mature teratoma-enriched lesions, and detected somatic mutations in 14 genes. However, no driver mutations were identified in the neuroblastoma-enriched sample. Conversely, recurrent copy number alterations, including +1q, +17, and −X, were identified, suggesting that these copy number alterations contributed to tumor development.

FIGURE 2 Genetic changes within the elements of the mature cystic teratoma and neuroblastoma by whole-exome sequencing and copy number analysis. A, Copy number analyses of neuroblastoma and teratoma lesions. Copy number plot from peripheral blood (upper panel), teratoma-enriched lesion (middle panel), and neuroblastoma-enriched lesion (lower panel) by a sequencing-based method. Note an allele-specific copy number of almost 1:1 in peripheral blood compared with genome-wide deviations from 1:1 in teratoma and neuroblastoma regions, demonstrating extensive LOH. B, Histograms of VAFs of 478 germline variants in a mature teratoma-enriched lesion (upper panel) and in a neuroblastoma-enriched lesion (lower panel). Mutations in each gene are shown in order sorted by the VAF value in the neuroblastoma lesion. Each mutated gene at the teratoma lesion is shown in the same order as at the neuroblastoma lesion

(A)

Peripheral blood

Mature teratoma-enriched lesion

Neuroblastoma-enriched lesion

(B)

Mature teratoma-enriched lesion

Neuroblastoma-enriched lesion
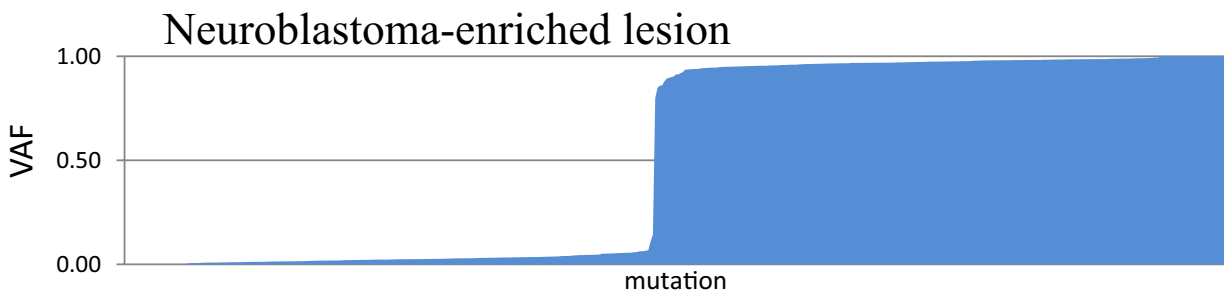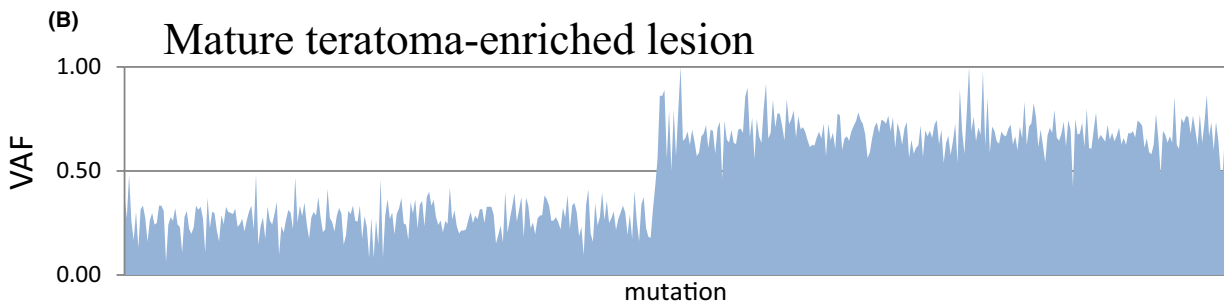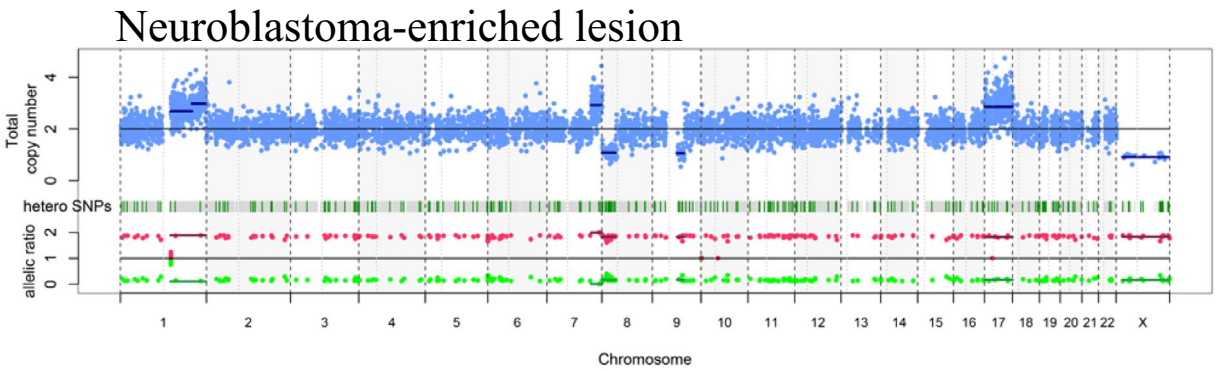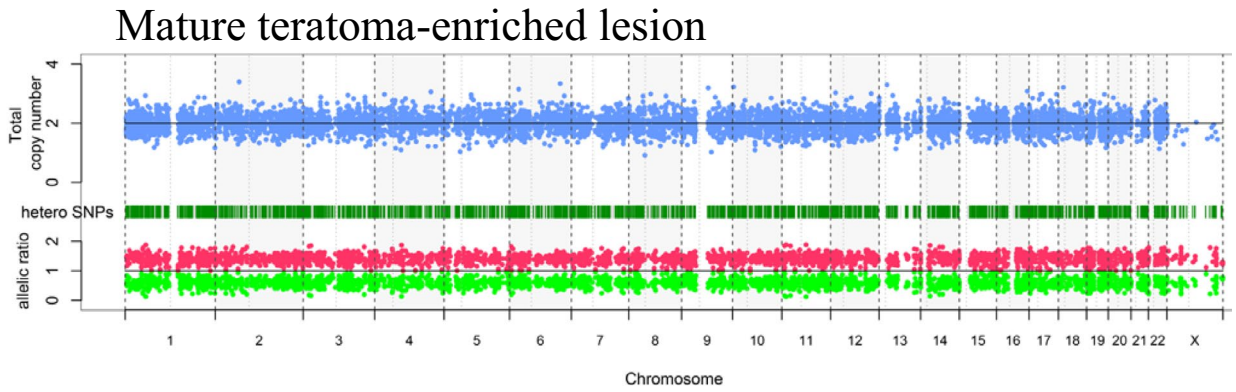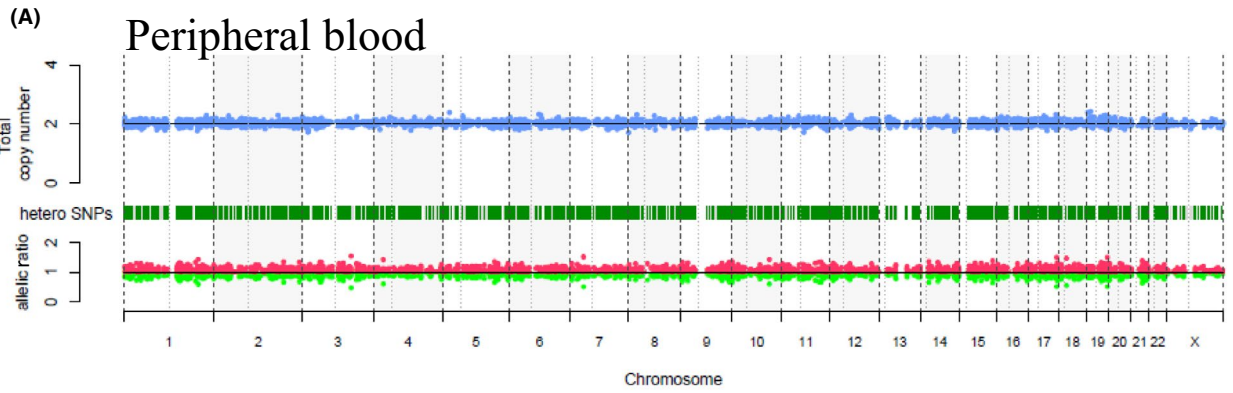
Copy number analysis also showed that the neuroblastoma-enriched sample and mature teratoma-enriched sample shared extensive CN-LOH. Genome-wide LOH and low frequencies of somatic mutations in teratomas are consistent with previous reports that found most teratomas were in a CN-LOH status because they arise from meiotic errors.[7-9] Furthermore, extensive CN-LOH has not been reported in neuroblastoma,[11] suggesting that neuroblastoma developed from teratoma cells. However, it is also possible that common ancestry clones characterized with CN-LOH generated both teratoma and neuroblastoma (Figure 3, alternative hypothesis). In addition, several heterozygous germline variants became homozygous because of extensive CN-LOH. For instance, a heterozygous nonsense mutation in *RBL2*, which has a known role in neural crest cell differentiation and cancer suppression,[12,13] detected in peripheral blood became homozygous in neuroblastoma. Similar findings were also observed in the epigenetic regulator *EZH2*[14] and tumor suppressor gene *FBXW12*.[15] These findings suggested that genome-wide LOH, which is a key pathognomonic change of a teratoma, may force heterozygous germline variants to become homozygous. Further investigation is mandatory to examine whether homozygous changes of tumor suppressor genes caused by genome-wide LOH may induce teratoma to acquire additional mutations or copy number alterations, which result in malignant transformation.

We experienced an adolescent case of mature teratoma-derived advanced neuroblastoma of the ovary. Considering the favorable outcome of our patient, teratoma-derived malignancies may have different biological characteristics compared with de novo malignancies. To our best knowledge, this is the 1st case in which a clonal relationship between teratoma and neuroblastoma was genetically confirmed. Furthermore, our results may suggest a possible mechanism of malignant transformation of teratomas, in which multiple heterozygous germline variants become homozygous because of genome-wide LOH, which is a hallmark cytogenetic abnormality of teratomas (Figure 3). Further studies to compare the genomic profiles of teratomas with and without malignant transformation are needed to elucidate tumorigenesis of somatic malignant neoplasms arising from teratomas.
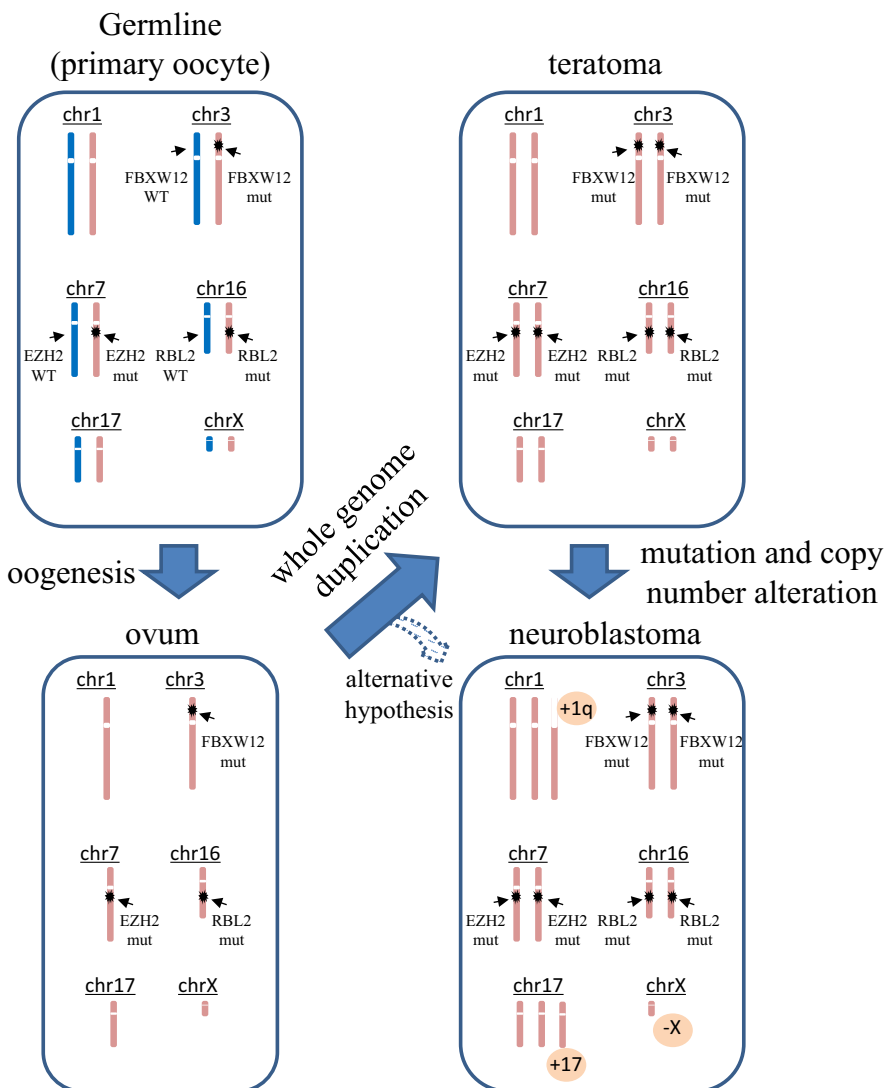

FIGURE 3 A model of malignant transformation from teratoma to neuroblastoma. A schematic diagram of tumorigenesis. During the process of oogenesis, germline cells (primary oocyte) become hemizygous. Errors in meiosis (whole genome duplication) lead to teratomas, in which heterozygous germline variants become homozygous. By acquiring additional mutations and/or copy number alterations, a part of the teratoma may develop neuroblastoma. Alternatively, common ancestry clones after whole genome duplication may independently develop to teratoma and neuroblastoma

ACKNOWLEDGMENTS

DISCLOSURE

The authors have no conflicts of interest.

ORCID

Rintaro Ono (iD) https://orcid.org/0000-0001-8847-2528

REFERENCES

1. Rathore R, Sharma S, Agarwal S. Malignant transformation in mature cystic teratoma of the ovary: a retrospective study of eight cases and review of literature. *Prz Menopauzalny Menopause Rev*. 2018;17:63-68.
2. Niwa Y, Yamamuro O, Kato N, Tsuzuki T. Two cases of primary ovarian neuroblastoma arising from mature cystic teratomas. *Gynecol Oncol Case Rep*. 2013;5:58-60.
3. Cooke SL, Ennis D, Evers L, et al. The driver mutational landscape of ovarian squamous cell carcinomas arising in mature cystic teratoma. *Clin Cancer Res*. 2017;23:7633-7640.
4. Mossé YP, Deyell RJ, Berthold F, et al. Neuroblastoma in older children, adolescents and young adults: a report from the International Neuroblastoma Risk Group project. *Pediatr Blood Cancer*. 2014;61:627-635.
5. Raetz EA, Kim MKH, Moos P, et al. Identification of genes that are regulated transcriptionally by Myc in childhood tumors. *Cancer*. 2003;98:841-853.
6. Zschüntzsch J, Schütze S, Hülsmann S, Dibaj P, Neusch C. Heterologous expression of a glial Kir channel (KCNJ10) in a neuroblastoma spinal cord (NSC-34) cell line. *Physiol Res*. 2013;62:95-105.
7. Kubota Y, Seki M, Kawai T, et al. Comprehensive genetic analysis of pediatric germ cell tumors identifies potential drug targets. *Commun Biol*. 2020;3:544.
8. Heskett MB, Sanborn JZ, Boniface C, et al. Multiregion exome sequencing of ovarian immature teratomas reveals 2N near-diploid genomes, paucity of somatic mutations, and extensive allelic imbalances shared across mature, immature, and disseminated components. *Mod Pathol*. 2020;33:1193-1206.
9. Shao L, Heider A, Rabah R. Single nucleotide polymorphism array and cytogenetic analyses of ovarian teratomas in children. *Genes Chromosom Cancer*. 2021;60(6):418-425.
10. Cheung NK, Zhang J, Lu C, et al. Association of age at diagnosis and genetic mutations in patients with neuroblastoma. *JAMA*. 2012;307:1062-1071.
11. Takita J, Hayashi Y, Kohno T, et al. Allelotype of neuroblastoma. *Oncogene*. 1995;11:1829-1834.
12. Raschellà G, Tanno B, Bonetto F, Negroni A, Amendola R, Paggi MG. Retinoblastoma family proteins induce differentiation and regulate B-myb expression in neuroblastoma cells. *Med Pediatr Oncol*. 2001;36:104-107.
13. Jori FP, Galderisi U, Piegari E, et al. RB2/p130 ectopic gene expression in neuroblastoma stem cells: evidence of cell-fate restriction and induction of differentiation. *Biochem J*. 2001;360:569-577.
14. Li Z, Takenobu H, Setyawati AN, et al. EZH2 regulates neuroblastoma cell differentiation via NTRK1 promoter epigenetic modifications. *Oncogene*. 2018;37:2714-2727.
15. Chen J, Hackett CS, Zhang S, et al. The genetics of splicing in neuroblastoma. *Cancer Discov*. 2015;5:380-395.

SUPPORTING INFORMATION

Additional supporting information may be found online in the Supporting Information section.